Scientific Research Publishing

Journal of Computer and Communications, 2024, 12, 241-262
https://www.scirp.org/journal/jcc
ISSN Online: 2327-5227
ISSN Print: 2327-5219

Low Complexity Digital Pre-Distortion (DPD) for Multi-Band Radio over Fiber Transmission Systems

Zijian Cheng, Xiupu Zhang

Department of Electrical and Computer Engineering, Concordia University, Montreal, Canada
Email: johnxiupu.zhang@concordia.ca

How to cite this paper: Cheng, Z.J. and Zhang, X.P. (2024) Low Complexity Digital Pre-Distortion (DPD) for Multi-Band Radio over Fiber Transmission Systems. *Journal of Computer and Communications*, **12**, 241-262.
https://doi.org/10.4236/jcc.2024.1211017

Received: November 12, 2024
Accepted: November 26, 2024
Published: November 29, 2024

Abstract

Nonlinear distortion is one of key limiting factors in radio over fiber (RoF) transmission systems. To suppress the nonlinear distortion, digital pre-distortion (DPD) has been investigated considerably. However, for multi-band signals, DPD becomes very complex, which limits the applications. To reduce the complexity, many simplified DPDs have been proposed. In this work, a new multidimensional DPD is proposed, in which in-band and out-of-band distortion are separated and the out-of-band distortion is evaluated by sum and differences of all input signals instead of all individual input signals, thus complexity is reduced. An up to 6-band 64-QAM orthogonal frequency division multiplexing (OFDM) signal with each bandwidth of 200 MHz in simulations and a 5-band 20 MHz 64-QAM OFDM signal in experiments are used to validate the proposed DPD. The validation is illustrated in the means of power spectrum, AM/AM and AM/PM distortion, and error vector magnitude (EVM) of the received signal constellations. The average EVM improvement by simulation for 3-band, 4-band, 5-band and 6-band signals is 19.97 dB, 18.65 dB, 16.64 dB and 15.44 dB, respectively. The average EVM improvement by experiments for 5-band signals is 8.1 dB. Considering the ten times of bandwidth difference, experiments and simulation agree well.

Keywords

Multidimensional, Digital Predistortion (DPD), Memorial Polynomial (MP), Power Amplifier (PA), Radio over Fiber, Fronthaul Networks, 5G

1. Introduction

With the rapidly increasing demand of high connectivity, the broadband wireless

transmission has been required. The fourth-generation mobile communication system (4G) has brought us a decent amount of speed and has offered us very high-quality online video and online gaming which benefit from its broadband. To meet continuing demand of wireless connectivity, the fifth-generation mobile communication system (5G) with new radio (NR) has been proposed and standardized, which advances massive device connectivity, high data rates, low latency, and sustainable cost.

The 5G access network consists of backhaul and fronthaul network. The existing fronthaul transmission technologies used for 3G and 4G may not be suitable for 5G [1], and alternatives such as frequency division multiple access (FDMA) and time-division multiple access (TDMA) based radio over fiber (RoF) may be more appropriate for 5G fronthaul networks [1]. Three key technologies for RoF fronthaul networks have been considered, *i.e.*, common protocol radio interface (CPRI) based digital radio over fiber (D-RoF), analog radio over fiber (A-RoF) and 1- or 2-bit delta-sigma modulation based radio over fiber (DSM-RoF). The D-RoF has digital optical transmission, but a complicated and high-cost remote antenna unit (RAU) is used, which induces a high-power consumption, and also the RF power amplifier in RAU requires complex broadband linearization [2]-[20]. The A-RoF has a simple RAU, but optical fiber transmission is analog, with which nonlinear distortion (such as harmonic and intermodulation distortion) is induced possibly by all online transmission components, thus much more complex broadband linearization is required [21]-[34]. The DSM-RoF has digital optical transmission, and also RAU is very simple, in which a simple broadband linearization may still be required [35]. Consequently, broadband linearization is required in all the three fronthaul transmission technologies.

Concurrent RF/millimeter-wave multi-bands will be used commonly in 5G, which increases the complexity of linearization significantly, and thus power consumption is increased accordingly.

Digital pre-distortion (DPD) is one of the key linearization techniques, which has been investigated considerably. Further, DPD techniques for linearization of multi-band signals have been developed with the focus on reducing complexity without significant sacrifice of linearization performance [2]-[20]. The currently reported low-complexity DPD models were almost all deduced from the conventional memorial Polynomial DPD with some approximations to reduce the number of terms. Moreover, more than three band DPDs have not been reported yet.

The first challenge for linearization of multi-band and/or a broadband signal is limited bandwidth of linearization. For a broadband signal or multiband signals, the pre-distorted signals require a wider bandwidth to include almost possible nonlinear distortion components that interfere with the signals, *i.e.* the pre-distorted signals need to have a wider bandwidth than the input signals. Under-sampling DPD [6] [13] and high-precision joint in-band/out-of-band DPD [2] are two methods to relieve this problem. Another way is to design a RoF or a power amplifier that supports broadband or multi-band signals [36] [37].

The second challenge for a broadband signal or multi-band signals are memory effect. Memory effect is increased with the signal bandwidth. The lagging and leading memory effect are two types of memory nonlinearities that may arise, and the output signal's memory extends to previous time instances. A technique introduced is to connect several quasi-Wiener-Hammerstein processes in parallel, which captures different aspects of the system's memory effect and can provide a better overall approximation of the system's behavior [38].

The third challenge is power consumption. The power consumption due to the high complexity DPD is considerable, and thus less-complexity DPD is preferred. Reduction of the complexity of DPD has been investigated [11] [12] [16]-[20]. For example, one method is combination of the cross-term-switching with the coefficient-switching [5], in which only the significant terms are considered that have large impact on nonlinear distortion. To reduce a strong memory effect induced complexity, a moving average nested general memory polynomial was proposed [39], improving the accuracy of envelope memorial polynomial by connecting several memory branches of envelope memorial polynomial in parallel. Further, a frequency shift technique was proposed to reduce complexity, in which 3rd and 5^{th} order intermodulation distortion (IMD3) (IMD5) influence on memory effect terms and nonlinearity terms are pre-calculated and used for evaluating an error until the desired performance is reached [18]. Alternatively, a pre-training assisted DPD was proposed that could reduce the complexity under the known nonlinearity [20]. Moreover, dynamic model sizing for a broadband DPD was demonstrated by sizing the unneeded coefficients to reduce the complexity [40].

In addition, to reduce the complexity of DPD, a broadband signal splitting into two or multi bands was proposed [41] [42]. To improve linearization accuracy, machine learning [4] [14] [15] [23] [28] and look-up table [9] have been proposed. To reduce sampling rates in DPD, a method with adjusting the group delay of signal samples and summing them up to cancel out the aliasing distortion was proposed [6] [13] [43].

As seen above, many efforts have been made to obtain less-complexity DPD with better accuracy for multi-band or multidimensional signals. In this work, a very simple DPD will be proposed for multi-band or multidimensional signals. Unlike the previously reported methods, the proposed approach has very limited increases of the DPD complexity with the increase of signal bands and the long-term memory effect.

2. Proposed Less-Complexity Multi-Band DPD

To illustrate the proposed DPD, the output y versus input x is given for a memoryless system by,

$$y = \sum_{k=0}^{K} a_k x^k \tag{1}$$

where a_k are the coefficients of the linearization function. K is the nonlinearity order of the linearization function. Note that even order nonlinear terms are not

located in band, thus for the simplicity, only odd orders will be taken only. To make the expression look more concise, the total nonlinearity orders of five (*K=5*) will be taken as an example. Therefore, (1) is reduced to

$$y = \sum_{k=0}^{2} a_{2k} x |x|^{2k} \tag{2}$$

Now, we consider a three-dimensional input signal as an example, *i.e.* the three-band input signal x is given by $x = x_1 e^{-j\omega_1 t} + x_2 e^{-j\omega_2 t} + x_3 e^{-j\omega_3 t}$. Thus, the output signal allocated at ω_1 is

$$\begin{aligned} y(\omega_1) = &\left(a_0 x_1 + a_2 x_1 \left(|x_1|^2 + |x_2|^2 + |x_3|^2 \right) \right. \\ &\left. + a_4 x_1 \left(|x_1|^4 + |x_2|^4 + |x_3|^4 + |x_2|^2 |x_3|^2 + |x_1|^2 |x_2|^2 + |x_1|^2 |x_3|^2 \right) \right) e^{-j\omega_1 t} \end{aligned} \tag{3}$$

For the output signals allocated at ω_2 and ω_3, they have the similar expressions as (3). Thus, we only take $y(\omega_1)$ as the example. To further simplify, (3) can be changed by considering the sum and difference of all input signals as follows,

$$\begin{aligned} &a_2 x_1 \left(|x_1|^2 + |x_2|^2 + |x_3|^2 \right) \\ &= 0.25 \times a_2 x_1 \left[\left(|x_1| + |x_2| + |x_3| \right)^2 + \left(|x_1| - |x_2| - |x_3| \right)^2 \right. \\ &\quad \left. + \left(|x_2| - |x_1| - |x_3| \right)^2 + \left(|x_3| - |x_2| - |x_1| \right)^2 \right] \end{aligned} \tag{4a}$$

$$\begin{aligned} &a_4 x_1 \left(|x_1|^4 + |x_2|^4 + |x_3|^4 + |x_2|^2 |x_3|^2 + |x_1|^2 |x_2|^2 + |x_1|^2 |x_3|^2 \right) \\ &= 0.25 \times a_4 x_1 \left[\left(|x_1| + |x_2| + |x_3| \right)^4 + \left(|x_1| - |x_2| - |x_3| \right)^4 \right. \\ &\quad \left. + \left(|x_2| - |x_1| - |x_3| \right)^4 + \left(|x_3| - |x_2| - |x_1| \right)^4 \right] \end{aligned} \tag{4b}$$

where we define

$$\begin{aligned} s_0 &= |x_1| + |x_2| + |x_3| \\ s_1 &= \left(|x_1| - |x_2| - |x_3| \right) \\ s_2 &= \left(|x_2| - |x_1| - |x_3| \right) \\ s_3 &= \left(|x_3| - |x_2| - |x_1| \right) \end{aligned} \tag{4c}$$

where s_0 is the sum of the all input signals, and s_1, s_2 and s_3 are the differences between the three input signals. With help of (4), (3) can be simplified, given by

$$y_1(n) = \sum_{k=0}^{K=2} \sum_{i=0}^{3} c_{k,i} x_1(n) s_i(n)^k + \sum_{k=0}^{K=2} d_k x_1(n) |x_1(n)|^k \tag{5}$$

where $c_{k,i}$ and d_k are the coefficients, $c_{k,i} = a_{k,i} / 4$, and $d_k = a_k$. K is the nonlinearity order and i denotes the numbers of s_i, i = 1, 2, 3, *i.e.* band number. Similarly, the output signals at ω_2 and ω_3 are given by

$$y_2(n) = \sum_{k=0}^{K=2} \sum_{i=0}^{3} c_{k,i} x_2(n) s_i(n)^k + \sum_{k=0}^{K=2} d_k x_2(n) |x_2(n)|^k \tag{6}$$

and

$$y_3(n)=\sum_{k=0}^{K=2}\sum_{i=0}^{3}c_{k,i}x_3(n)s_i(n)^k+\sum_{k=0}^{K=2}d_k x_3(n)\left|x_3(n)\right|^k \quad (7)$$

respectively. Using the similarity of (5)-(7), we can deduce the output for multi-band signals. By adding memory effect, the l_{th} band output $y_l(n)$ for the multi-band input $x_l(n)$ is given by,

$$\begin{aligned}y_l(n)=&\sum_{m=0}^{M}\sum_{k=0}^{K}\sum_{i=0}^{L}c_{l,m,k,i}x_l(n-m)s_{l,i}^k(n-m)\\&+\sum_{m=0}^{M}\sum_{k=0}^{K}d_{l,m,k}x_l(n-m)\left|x_l(n-m)\right|^k\end{aligned} \quad (8)$$

where $l = 1, 2, \ldots, L$, and L denotes the total band of input signals, $s_{l,i}$ is the sum and difference of all different bands, M and K are the memory depth and the non-linearity order, respectively. s_i for multi-bands is given as

$$\begin{aligned}s_0&=|x_1|+|x_2|+\cdots+|x_L|\\s_1&=|x_1|-|x_2|-\cdots-|x_L|\\s_2&=|x_2|-|x_1|-\cdots-|x_L|\\&\cdots\\s_L&=|x_L|-|x_1|-\cdots-|x_{L-1}|\end{aligned} \quad (9)$$

The expression (8) is the general form for the newly proposed low-complexity DPD model, which can be considered as a *modified memorial Polynomial DPD*. Note that the newly proposed DPD given by (8) is obtained from the conventional memorial Polynomial DPD without any approximations, but the expression form is changed, in which the sum and differences of all input signals are used to calculate out-of-band (or cross-of-band) distortion (1st term of (8)) instead of all individual input signals. Thanks to calculation of the out-of-band distortion by use of the sum and differences of all input signals, the number of coefficients that are needed for the newly proposed DPD model is reduced significantly. The second term of (8) represents the in-band nonlinear distortion.

3. Simulation and Results

All simulations are performed on Matlab. The purpose of the simulations is to understand the performance of the DPD proposed in this work.

The input signal is mapped into 64 QAM symbols. The 200 MHz baseband signal is allocated by those symbols and inverse fast Fourier transform is used to map into orthogonal-frequency-division-multiplexing (OFDM) signals. Then, the signal is transmitted into the DPD model to produce the pre-distorted signals.

The pre-distorted signals pass through an RoF link which introduces nonlinear distortion due to electrical and optical components. The RoF is emulated by a Wiener-Hammerstein nonlinear transmission model, which was built by two linear filters with a static nonlinearity polynomial block in the middle [44]. Finally, the received signals will be fed back into the DPD model to further optimize the

DPD coefficients and then the DPD performance is analyzed to determine whether the DPD model (coefficients) needs the further optimization.

To have the DPD work well, the optimal nonlinearity order and memory depth must be set properly, which depend on the considered RoF transmission system. Error vector magnitude (EVM) is an indicator used to observe the in-band distortion. So EVM is used to determine the optimal nonlinearity order and memory depth that make the DPD work properly.

Here we consider three bands at 1.05 GHz, 1.53 GHz and 2.1 GHz, and each has a 200 MHz bandwidth to find the best nonlinearity order and memory depth.

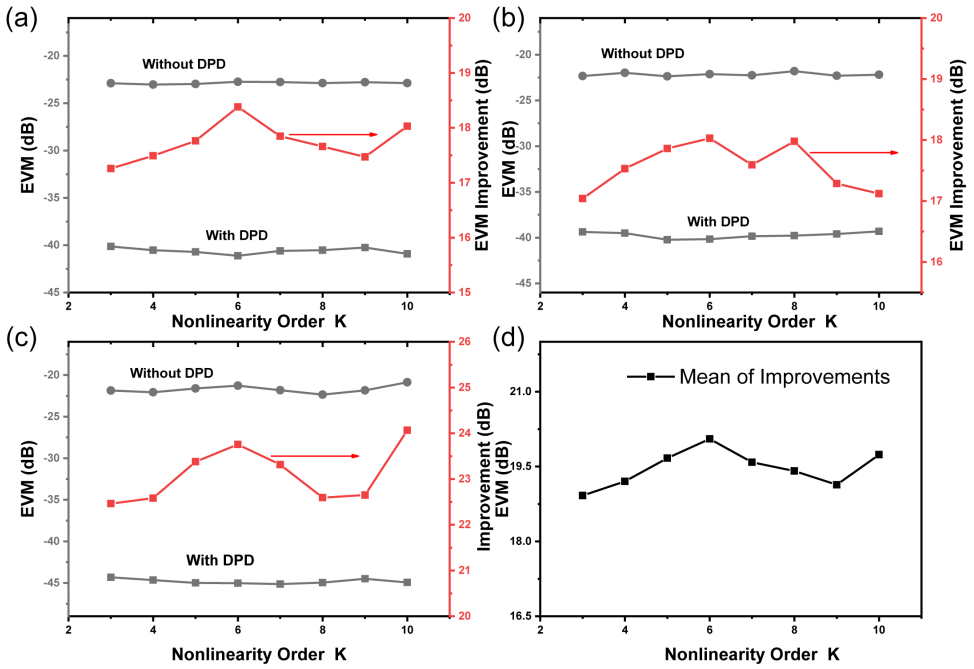

Figure 1. EVM vs nonlinearity order for (a) 1st band (a), (b) 2nd band, (c) 3rd band, and (d) mean of improvements of three bands.

Figure 1 presents the relationship between EVM and nonlinearity order at memory depth $M = 7$. **Figures 1(a)-(c)** are the results of simulated EVM for the two cases: without and with the proposed DPD for each band, and **Figure 1(d)** is the mean of the improvements of the three bands by using the proposed DPD. As can be seen, the improvement becomes better till a peak for each band as the nonlinearity order increases. The peak occurs at the nonlinearity order $K = 6$, and also the other peak occurs at $K = 10$ for the first and third band. Considering the complexity of the DPD, nonlinearity order $K = 6$ is chosen since the best performance at $K = 6$ is achieved.

Now consider the impact of the memory depth, and the same three bands are taken into consideration. Here nonlinearity order $K = 6$ is always assumed. The memory depth is ranged from one to ten. **Figure 2** shows the mean EVM improvement of the three bands by the proposed DPD. It is obvious that the improvement starts saturated as the memory depth increases after three, and then it

becomes relatively saturated. Thus, the memory depth $M = 5$ that will be used later should be enough.

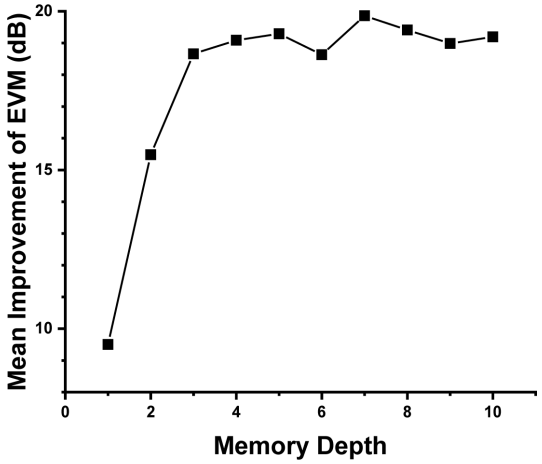

Figure 2. Mean improvement of EVM for the three bands versus memory depth.

Next, we use the above DPD for six bands of the input signal, and the six bands are at 1.05, 1.53, 2.1, 2.83, 3.52, and 4.02 GHz. Each band has a bandwidth of 200 MHz. The input signal is generated randomly by MATLAB and used to build OFDM waveform.

Figure 3 shows simulated power spectrum for the six band signals for the cases of with and without the proposed DPD. It is seen that the nonlinear distortion in the out-of-band of the signal is severe when without the DPD applied. With the application of the proposed DPD, the out-of-band nonlinear distortion is suppressed considerably. The average adjacent channel power ratio (ACPR) improvement is around 14 dB. For the in-band suppression, it is not very clear from the spectrum. Correspondingly, **Figure 4** shows the signal constellations, which are more distorted by in-band distortion, for the two cases: Left and right signal constellation showing the cases without and with the proposed DPD for the six bands (from top to bottom: 1st to 6th band). The improvement of EVM for the six bands is 13.33, 13.05, 14.31, 15.48, 17.46, and 19.02 dB. The average improvement of EVM for all the six bands is around 15.44 dB.

To further show performance of the proposed DPD, AM/AM (AM: amplitude modulation) and AM/PM (PM: phase modulation) distortion for without and with the proposed DPD are compared in **Figure 5** for the six bands. It is observed that both AM and PM linearity are improved significantly.

Table 1 presents a summary of EVM improvement using the proposed DPD used for three, four, five, and six bands of signal.

Because the memorial Polynomial DPD for multiband signals is much complicated and not possibly implemented for more than three bands. For a fair comparison with this proposed DPD, we consider the band-by-band DPD technique for multi-band signals. With this approach, separate single-band DPDs are trained and applied to each individual band of the multi-band signals. Once the individual

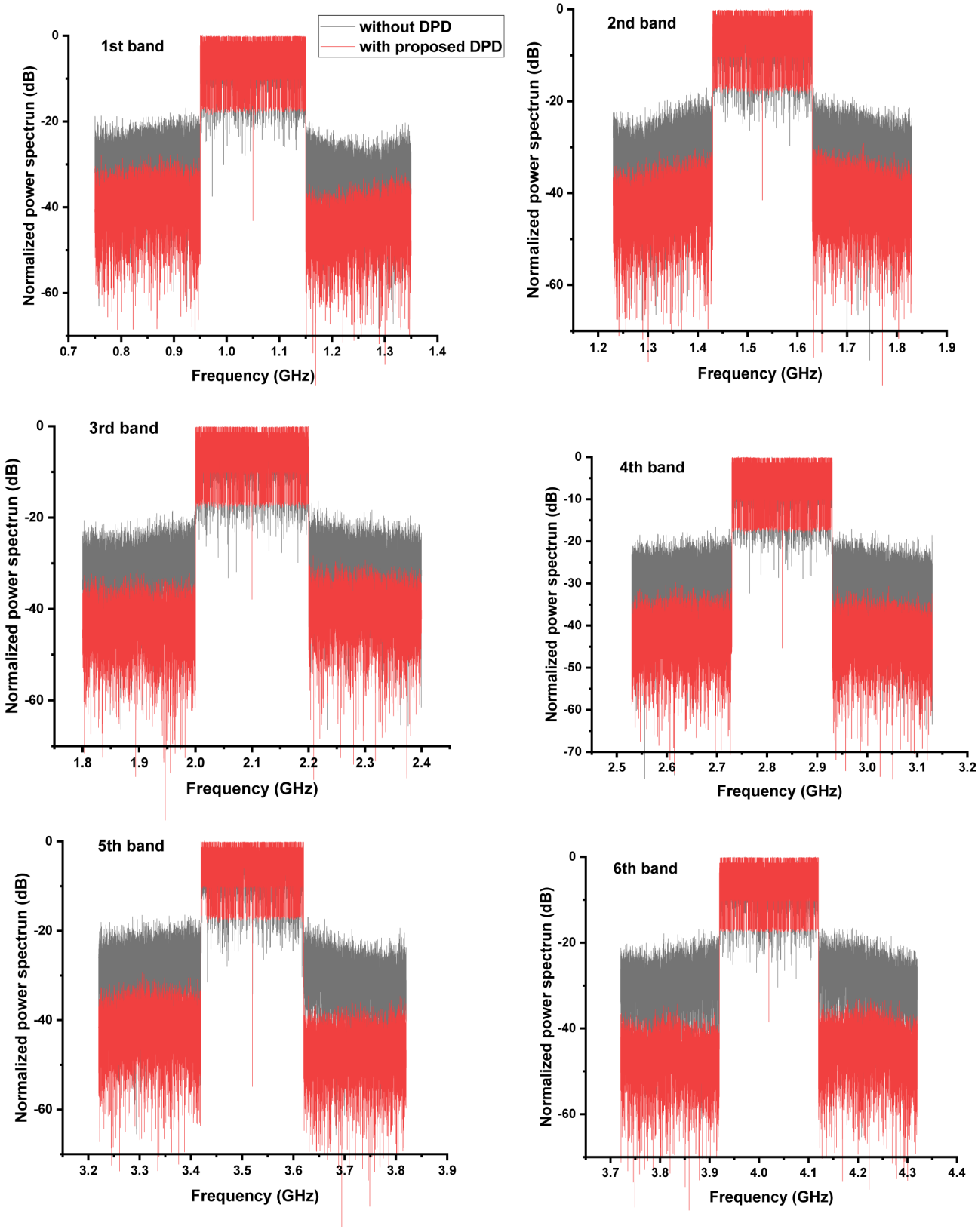

Figure 3. Normalized power spectrum for six band signals. Top to bottom: 1st to 6th band. Black: without DPD and Red: with the proposed DPD.

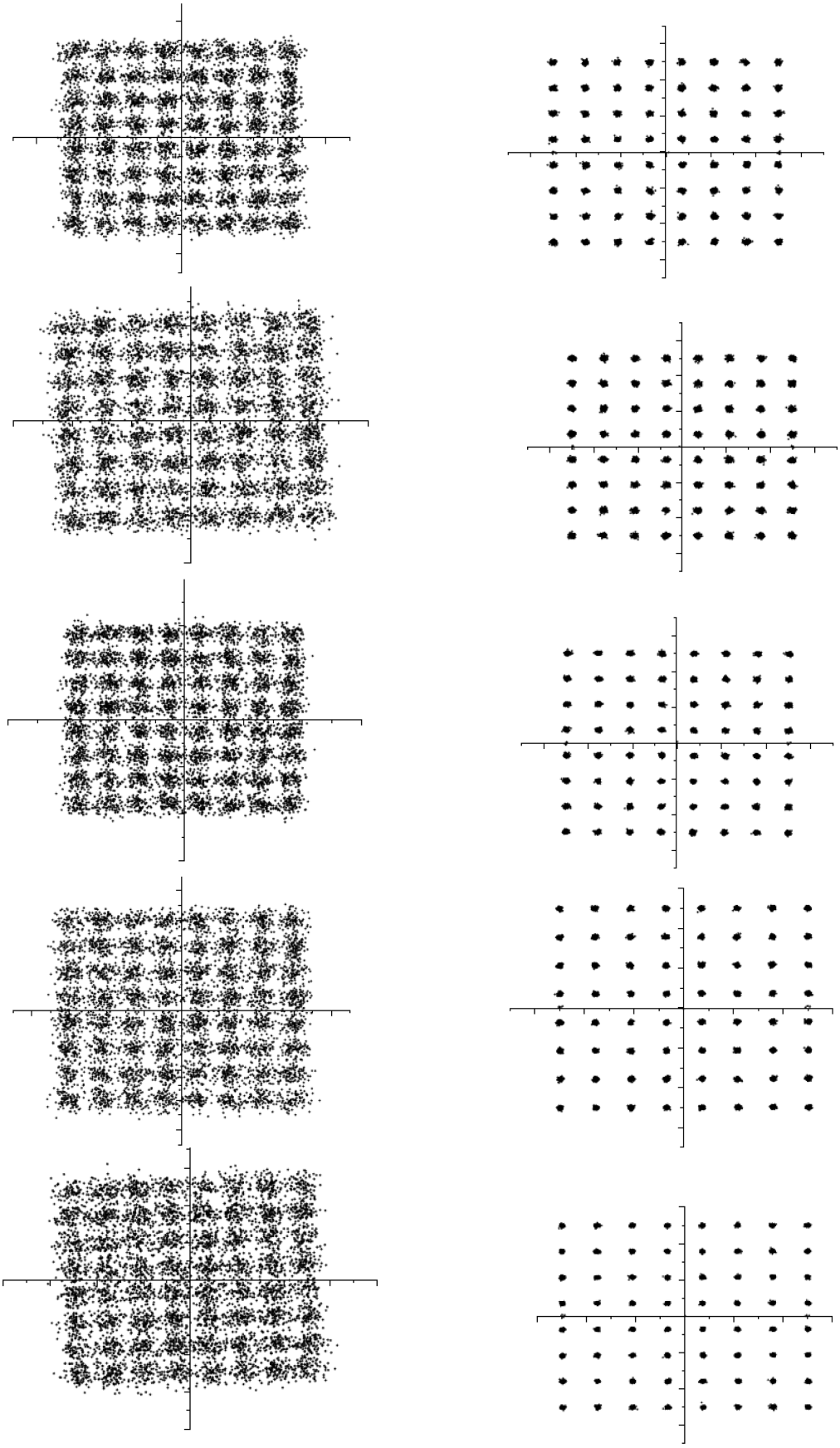

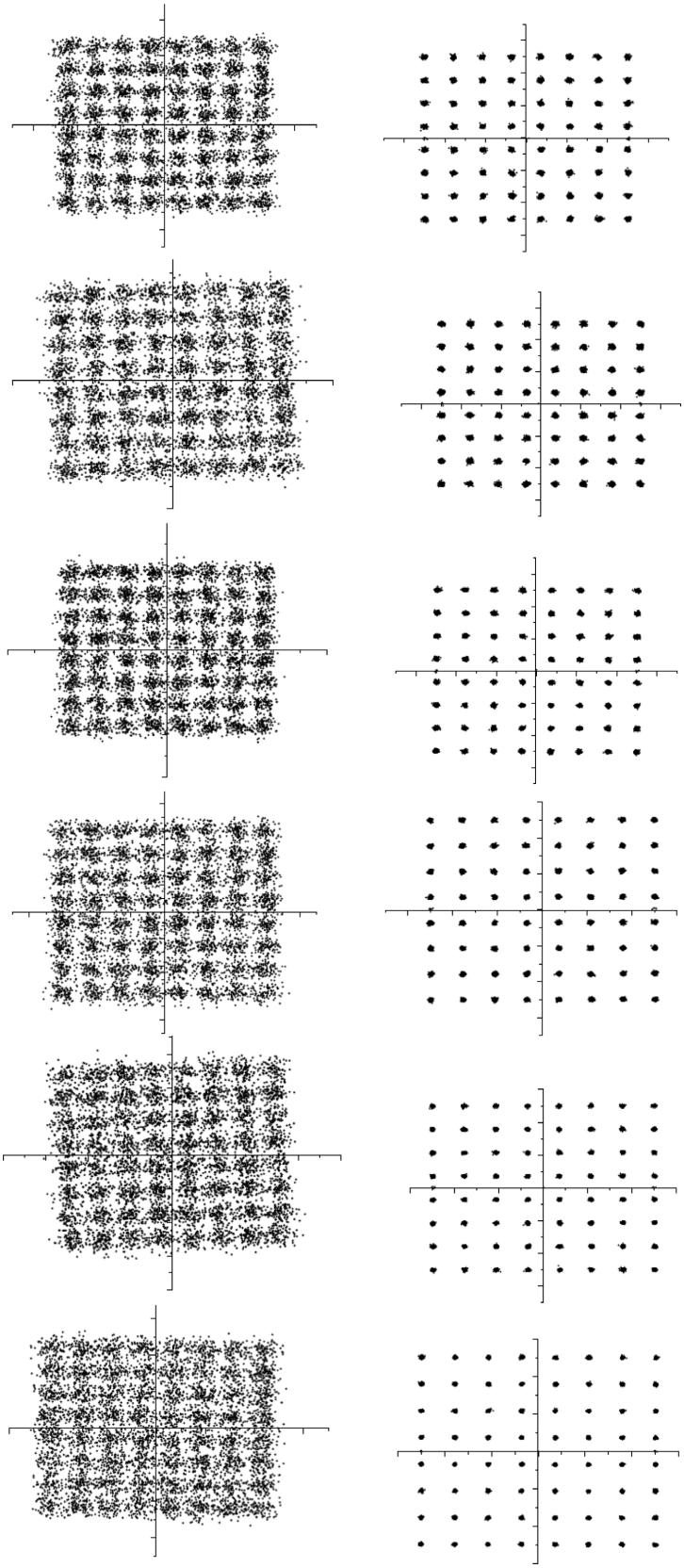

Figure 4. Constellation of the six band signals. Left: without DPD, and right: with the proposed DPD. From top to bottom: 1st to 6th band.

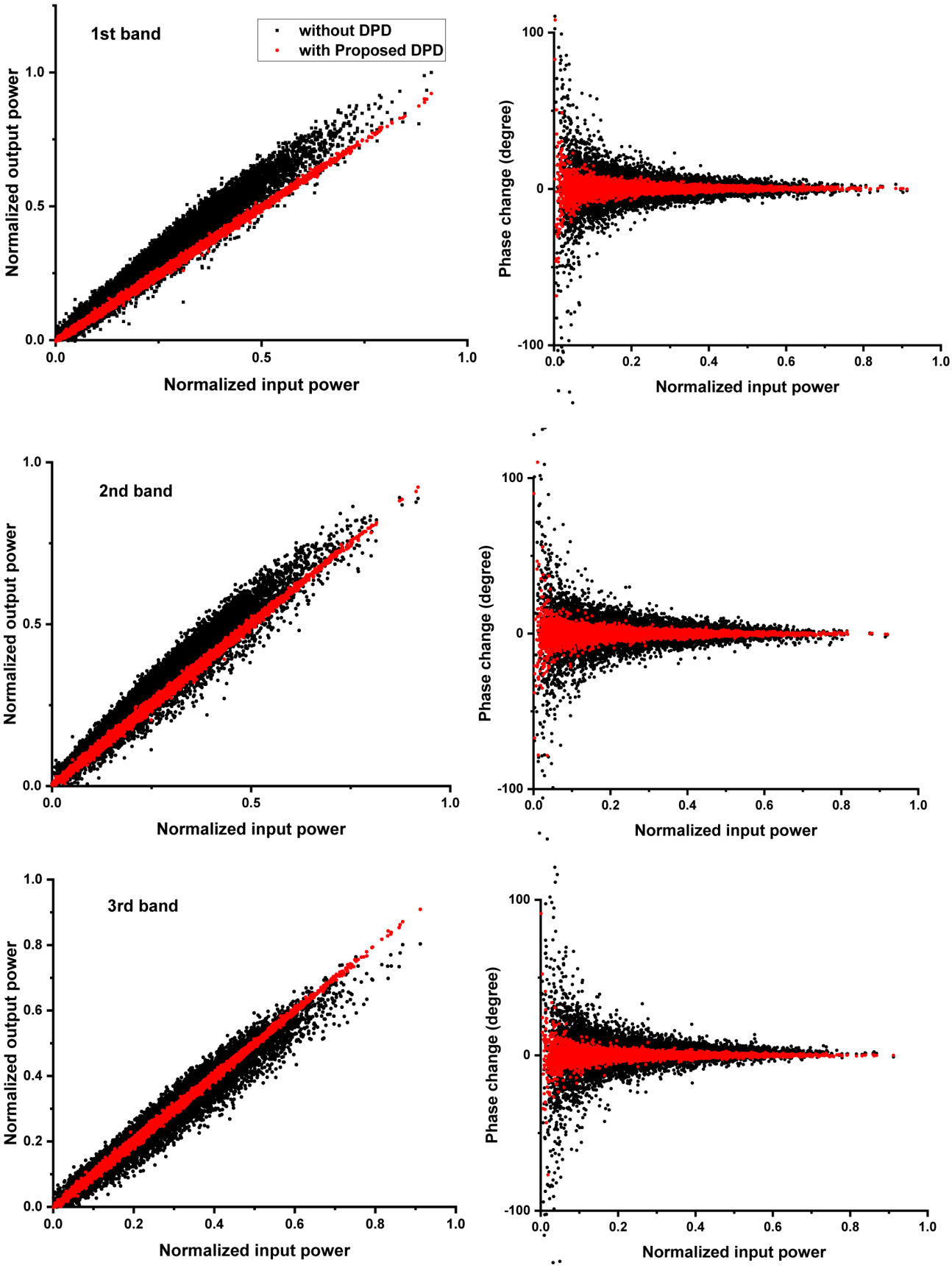
1st band
without DPD
with Proposed DPD
Normalized output power
Normalized input power
Phase change (degree)
Normalized input power
2nd band
Normalized output power
Normalized input power
Phase change (degree)
Normalized input power
3rd band
Normalized output power
Normalized input power
Phase change (degree)
Normalized input power

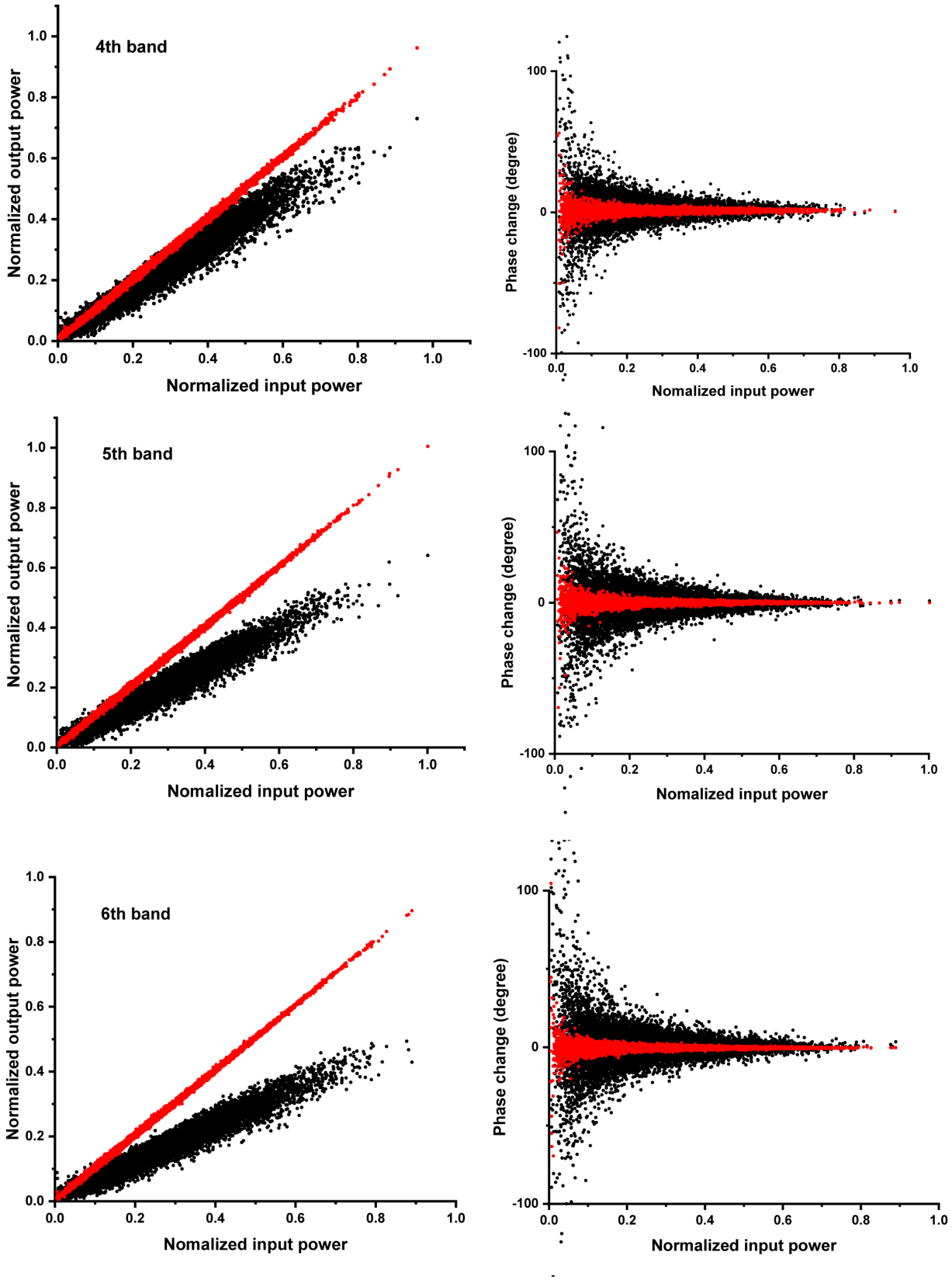

Figure 5. AM/AM and AM/PM distortion of the six band signals for the cases without and with the proposed DPD. Up to bottom: 1st band to 6th band.

Table 1. EVM improvement by the proposed DPD.

Bands	Mean improvement (dB)
3	19.97
4	18.65
5	16.64
6	15.44

bands are processed using the single-band DPD, the resulting signals are combined to form the final multi-band signals. Note that for the band-by-band DPD, the nonlinear distortion within each individual band, *i.e.* in-band distortion, is included only, while the potential nonlinear distortions from other bands, *i.e.* out-of-band distortion, are not included. The simulation shows that the average improvement of this band-to-band DPD is 13.93 dB for three, four and five bands of signals, thus 4.5 dB worse than the proposed DPD.

4. Experimental Validation

The experimental setup is shown in **Figure 6**. The 64-QAM OFDM signal is generated in Matlab and then loaded into a Tektronix AWG7122B arbitrary waveform generator (AWG). The AWG sends the signals to the optical transmitter at a sampling rate of 10.32 Giga samples per second (GS/s). A MITEQ SCM fiber optic link is used to transmit and receive the optical signal. The optical transmitter is a direct modulated laser, which contains a pre-amplifier boosting the input signal at bias of 12 V and −12 V. After the modulated optical signal passing through an 8-kilometer standard single mode optical fiber, which has a total 13 dB attenuation, the optical signal is detected by the optical receiver of the MITEQ SCM fiber optical link and demodulated back into an RF signal. An SHF810 broadband amplifier is connected after the optical receiver to enhance the power level of the RF signal from −15.4 dBm to 13.4 dBm, corresponding to a gain of 28 dB (not saturated). An Agilent DSO81204B oscilloscope samples the amplified RF signal at a sampling rate of 10.32 GS/s and saves the data into a file, which can be processed by Matlab. The optical power at fiber input is about 7 dBm at 1550 nm.

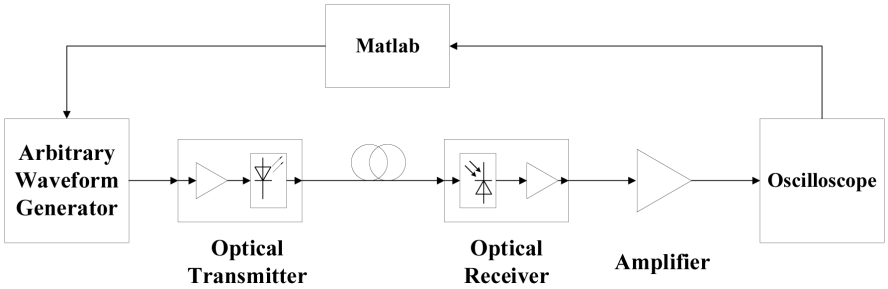

Figure 6. Experimental setup.

Here we consider five bands, which are located at 720, 800, 845, 900 and 960 MHz. Each band has a bandwidth of 20 MHz, instead of 200 MHz in simulation. The

memory depth $M = 5$ and nonlinearity order $K = 6$ are set for the DPD function.

Figure 7 shows the measured power spectrum for all the five bands for the two

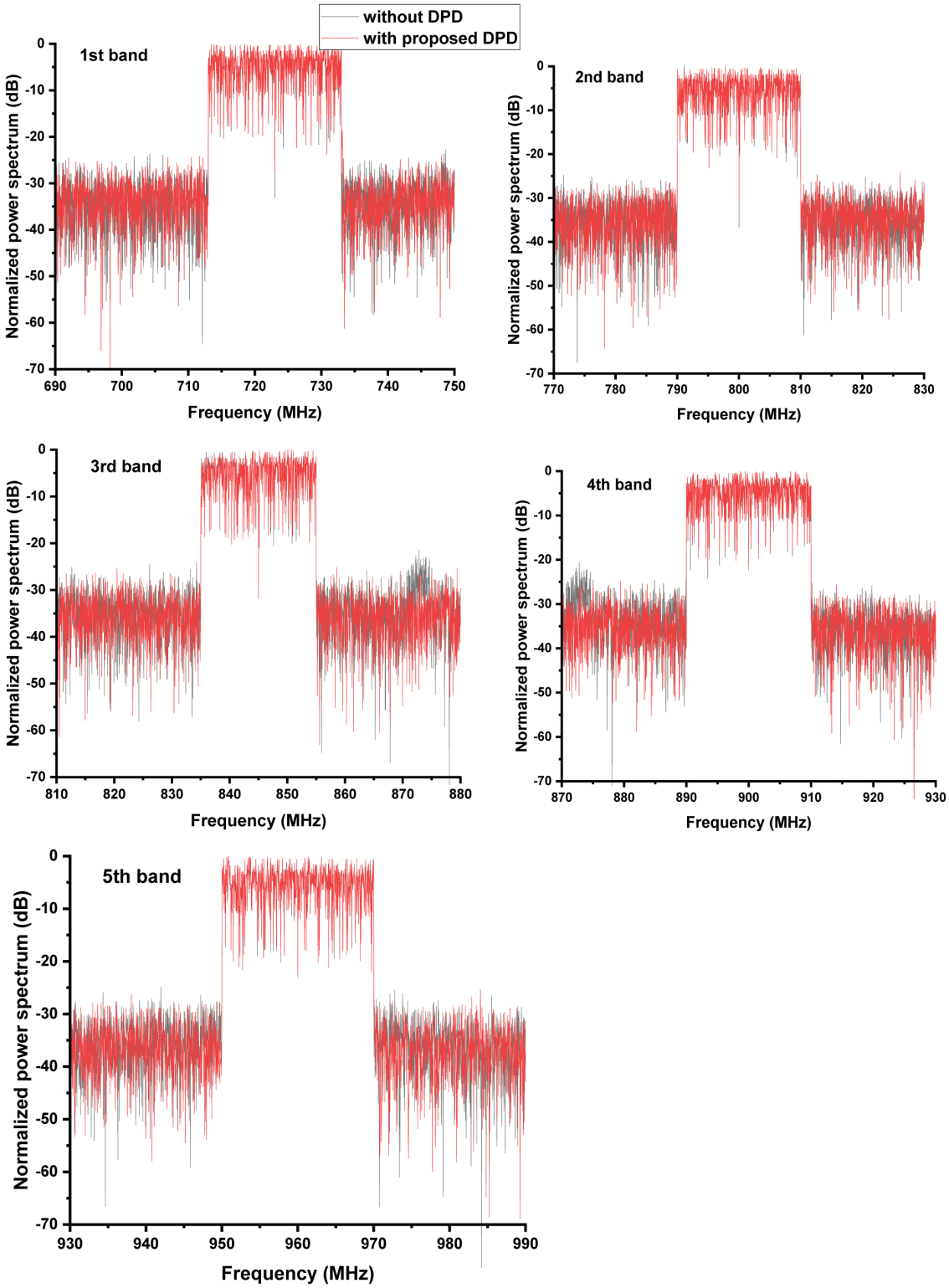

Figure 7. Measured power spectrum for the five bands (from top to bottom: 1st to 5th band) for the two cases of without (black) and with the proposed DPD (red).

cases of without and with the proposed DPD. It is seen that the nonlinear distortion is suppressed. Since this RoF transmission system does not have severe nonlinearities, the suppression by the DPD is not considerable. Correspondingly, the measured AM/AM and AM/PM distortion are illustrated in **Figure 8**. It is seen

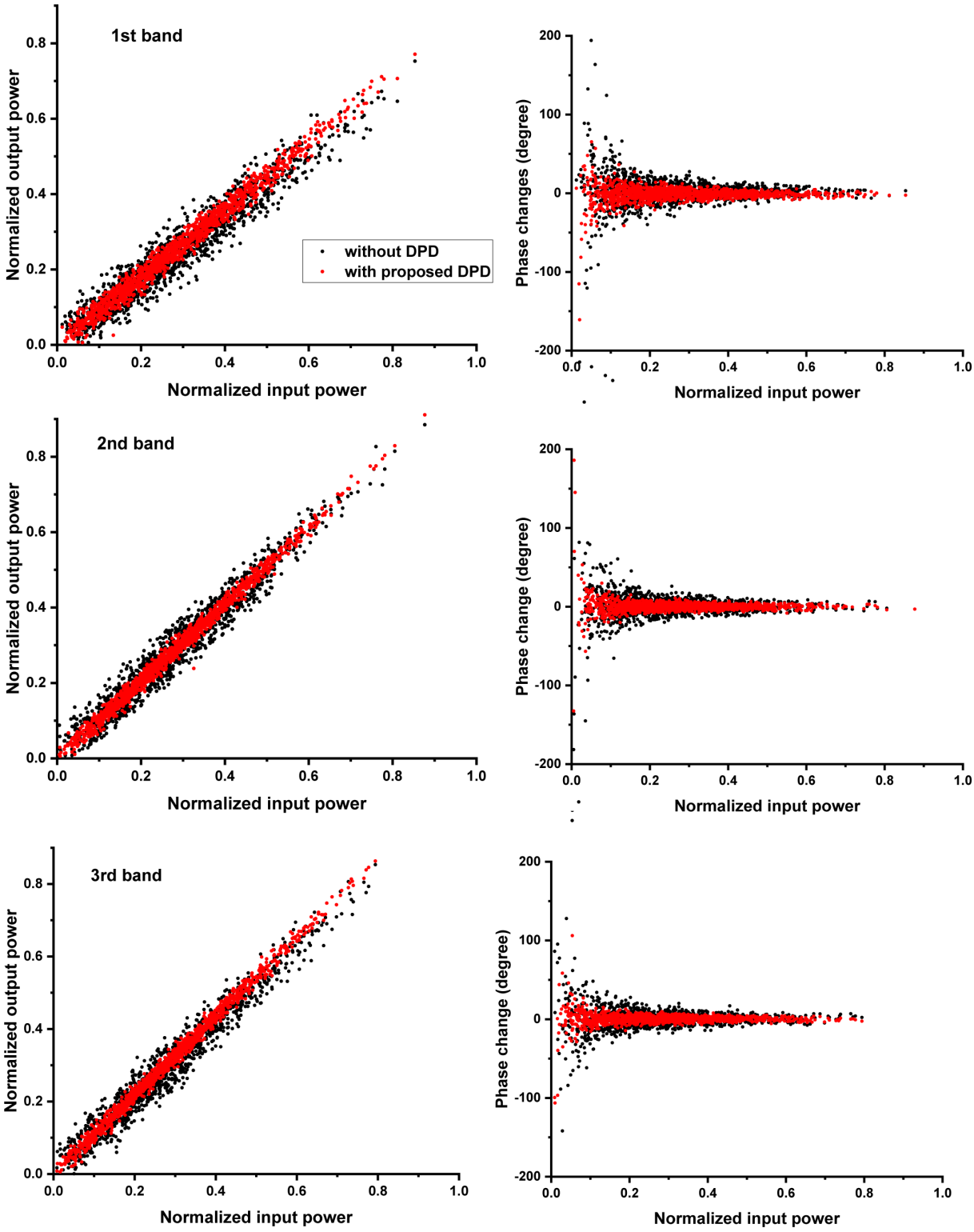

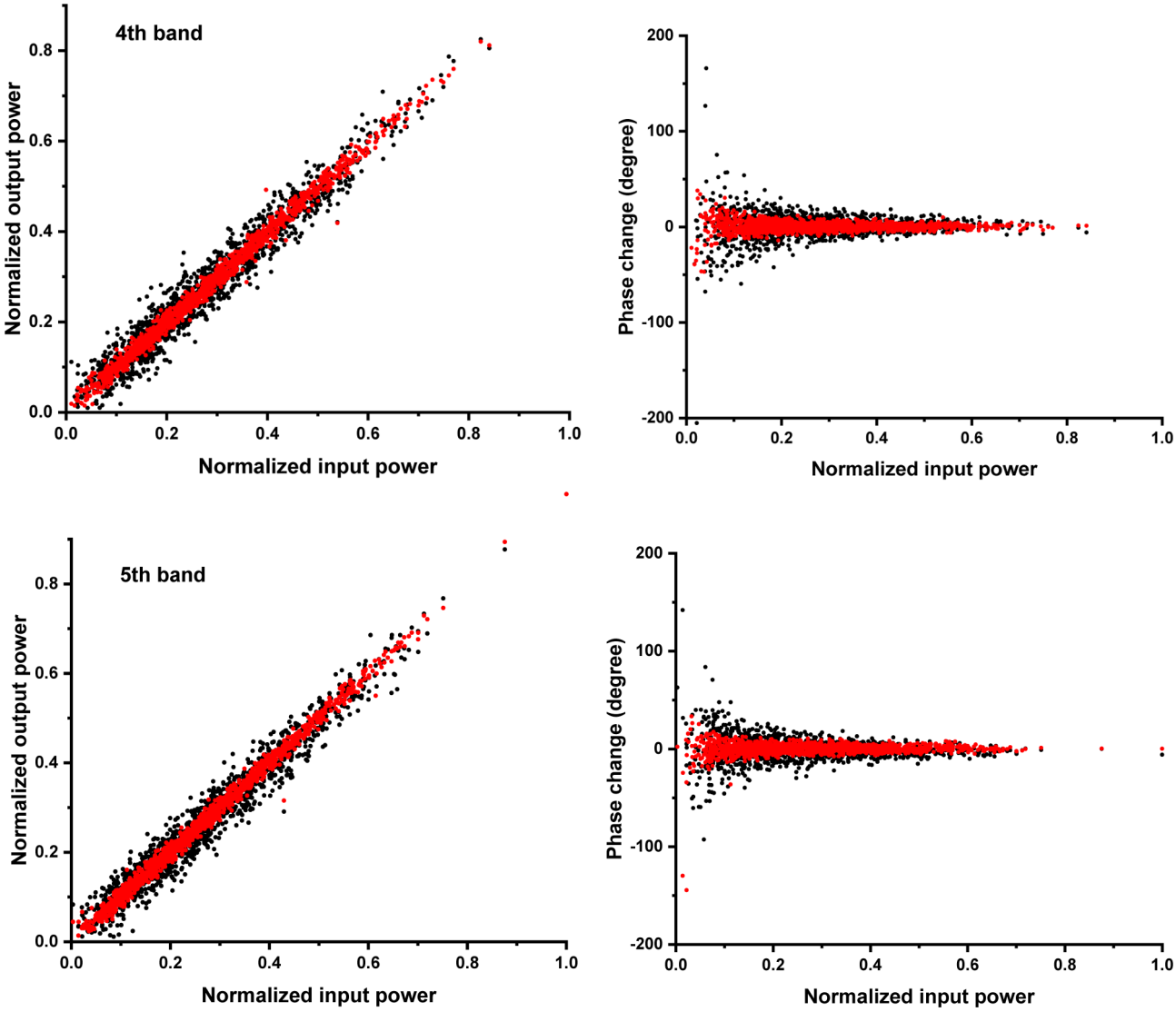

Figure 8. Measured AM/AM (left) and AM/PM (right) distortion after RoF transmission for the two cases of without (black) and with the proposed DPD (red) for the five bands (top to bottom: 1st to 5th band).

that the proposed DPD improves the linearity of AM/AM and AM/PM distortion obviously.

Figure 9 shows the measured signal constellations of the five bands for RoF transmission system without and with the proposed DPD. Corresponding to **Figure 9**, the improvement of EVM for the five bands is summarized in **Table 2**. For all the five bands, the average EVM improvement is 8.1 dB. Considering the ten times of bandwidth difference compared to the simulation, EVM improvement from simulation and experiments agrees fairly.

Table 2. EVM improvement for the five bands using the proposed DPD.

Band	1	2	3	4	5
Improvement	8.6	8.1	8.1	7.1	7.9

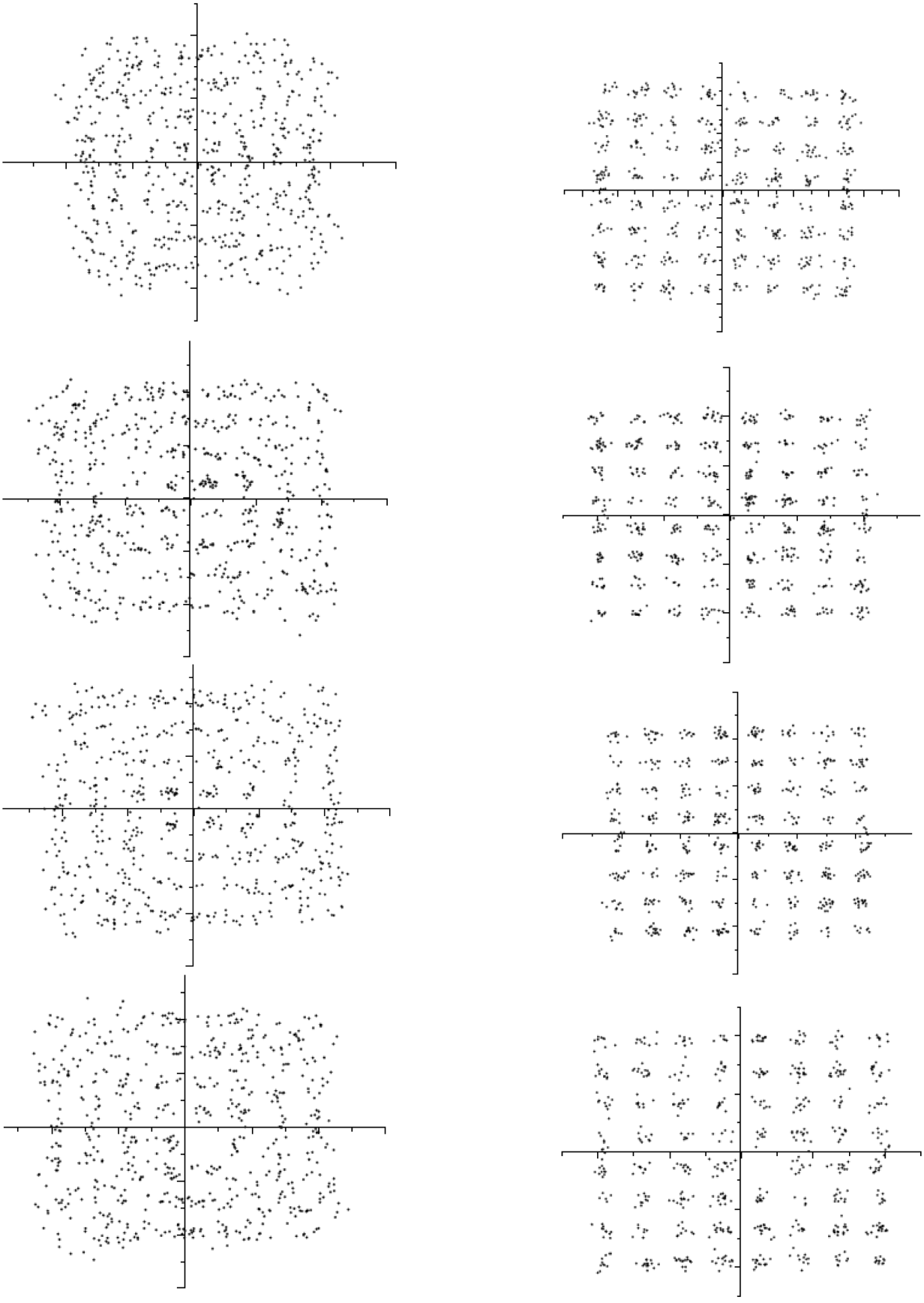

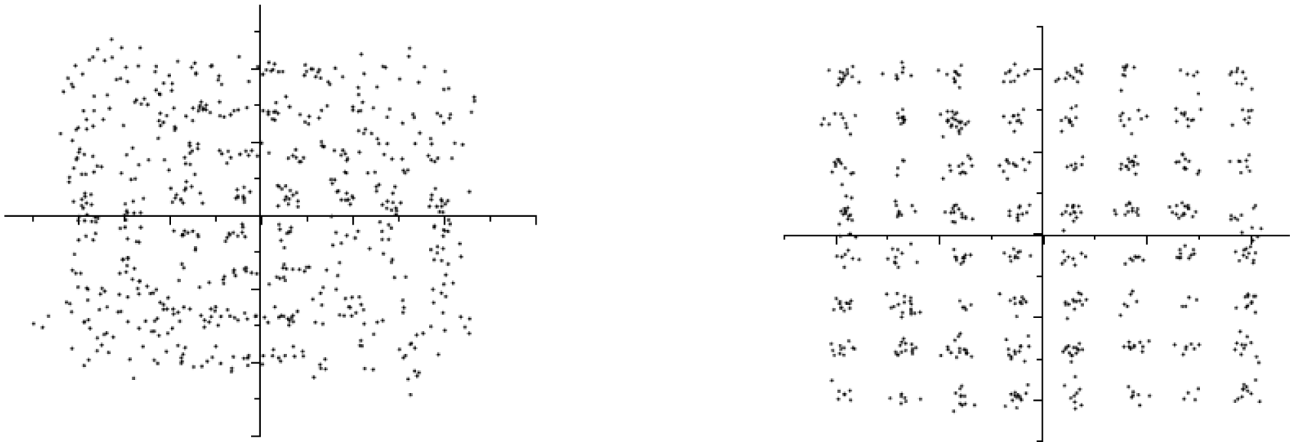

Figure 9. Measured signal constellations of the five bands for the cases of without (left) and with the proposed DPD (right). Top to bottom: 1st to 5th band.

4. DPD Complexity and Accuracy

The complexity of a DPD is represented by the number of coefficients that are used for the DPD model. **Figure 10(a)** and **Figure 10(b)** show the number of coefficients versus nonlinearity order for memory depth of six ($M = 6$) for three and six bands of input signals, respectively. It is seen that the complexity of the conventional memory Polynomial DPD increases exponentially with the increase of nonlinearity order. However, the proposed new DPD increases slightly in a roughly linear scale. With the increase of signal bands, such as 6 bands, the proposed new DPD will introduce more reduction in DPD complexity as shown in **Figure 10(b)**. For example, the number of coefficients is 3696 and 384 for the conventional and our proposed new DPD, respectively for $M = 6$ and $K = 6$.

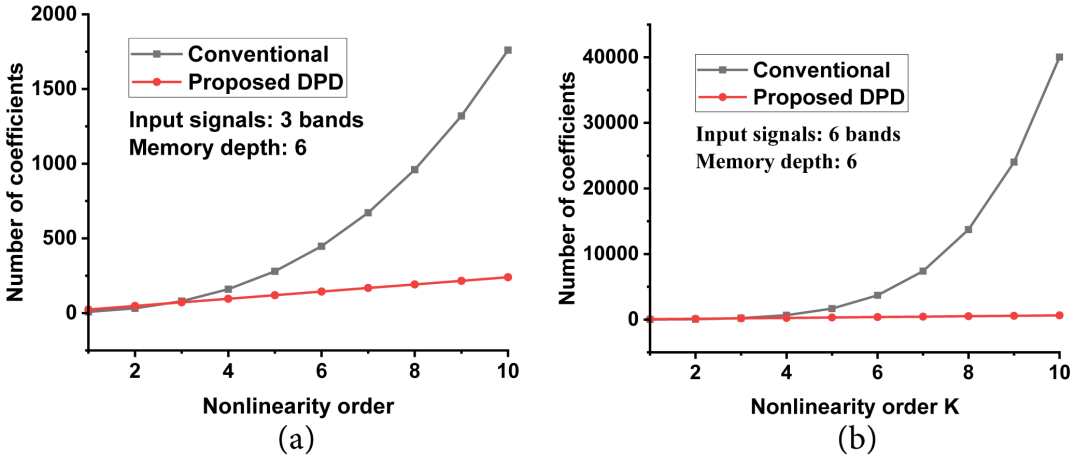

Figure 10. Comparison of the number of coefficients versus nonlinearity order for (a) 3 and (b) 6 bands of signal. Memory depth of $M = 6$ is used.

As is mentioned that the new DPD given by (8) is directly deduced from the conventional memory Polynomial DPD *without any approximations*, in which the out-of-band distortion is computed by the sum and differences of all input

signals instead of all individual input signals, thus the complexity is reduced. Therefore, the difference of the new and conventional DPD is the expression form only, thus the accuracy of them should be the very similar. The detailed comparison is required to further study.

5. Conclusion

We have proposed a low-complexity DPD for multi-band of signals. The new DPD is deduced directly from the conventional DPD without any approximations. The in-band and out-of-band distortion are separated in the newly proposed DPD and the out-of-band distortion is calculated by the sum and differences of all input signals instead of all individual input signals, and thus the complexity is reduced significantly. The newly proposed DPD was validated by simulation and experiments. The measured mean improvement of EVM is 8.1 dB for five-band 20 MHz 64-QAM OFDM signal over an 8-km RoF link. Both simulation and experiments have shown that the newly proposed DPD suppresses both in-band and out-of-band distortion well.

Conflicts of Interest

The authors declare no conflicts of interest regarding the publication of this paper.

References

[1] Zhang, X. (2018) Broadband Linearization for 5G Fronthaul Transmission. *Frontiers of Optoelectronics*, **11**, 107-115. https://doi.org/10.1007/s12200-018-0802-4

[2] Yu, C., Yang, N., Lu, Q., Cai, J. and Zhu, X. (2018) High-Precision Joint In-Band/Out-of-Band Distortion Compensation Scheme for Wideband RF Power Amplifier Linearization. *IEEE Microwave and Wireless Components Letters*, **28**, 1044-1046. https://doi.org/10.1109/lmwc.2018.2867094

[3] Suo, Y., Qiao, W., Jiang, C., Zhang, B. and Liu, F. (2022) A Residual-Fitting Modeling Method for Digital Predistortion of Broadband Power Amplifiers. *IEEE Microwave and Wireless Components Letters*, **32**, 1115-1118. https://doi.org/10.1109/lmwc.2022.3162759

[4] Hongyo, R., Egashira, Y., Hone, T.M. and Yamaguchi, K. (2019) Deep Neural Network-Based Digital Predistorter for Doherty Power Amplifiers. *IEEE Microwave and Wireless Components Letters*, **29**, 146-148. https://doi.org/10.1109/lmwc.2018.2888955

[5] Li, Y., Wang, X. and Zhu, A. (2022) Reducing Power Consumption of Digital Predistortion for RF Power Amplifiers Using Real-Time Model Switching. *IEEE Transactions on Microwave Theory and Techniques*, **70**, 1500-1508. https://doi.org/10.1109/tmtt.2021.3132347

[6] Peng, J., You, F. and He, S. (2022) Under-Sampling Digital Predistortion of Power Amplifier Using Multi-Tone Mixing Feedback Technique. *IEEE Transactions on Microwave Theory and Techniques*, **70**, 490-501. https://doi.org/10.1109/tmtt.2021.3110237

[7] Jindal, G., Watkins, G.T., Morris, K. and Cappello, T.A. (2022) Digital Predistortion of RF Power Amplifiers Robust to a Wide Temperature Range and Varying Peak-to-Average Ratio Signals. *IEEE Transactions on Microwave Theory and Techniques*, **70**,

3675-3687. https://doi.org/10.1109/tmtt.2022.3175155

[8] Li, C., He, S., You, F., Peng, J. and Hao, P. (2020) Analog Predistorter Averaged Digital Predistortion for Power Amplifiers in Hybrid Beam-Forming Multi-Input Multi-Output Transmitter. *IEEE Access*, **8**, 146145-146153. https://doi.org/10.1109/access.2020.3013965

[9] Pham, Q.A., Lopez-Bueno, D., Wang, T., Montoro, G. and Gilabert, P.L. (2018) Partial Least Squares Identification of Multi Look-Up Table Digital Predistorters for Concurrent Dual-Band Envelope Tracking Power Amplifiers. *IEEE Transactions on Microwave Theory and Techniques*, **66**, 5143-5150. https://doi.org/10.1109/tmtt.2018.2857819

[10] Yu, C., Tang, K. and Liu, Y. (2020) Adaptive Basis Direct Learning Method for Predistortion of RF Power Amplifier. *IEEE Microwave and Wireless Components Letters*, **30**, 98-101. https://doi.org/10.1109/lmwc.2019.2951193

[11] Yu, C., Lu, Q., Yin, H., Cai, J., Chen, J., Zhu, X., *et al.* (2020) Linear-Decomposition Digital Predistortion of Power Amplifiers for 5G Ultrabroadband Applications. *IEEE Transactions on Microwave Theory and Techniques*, **68**, 2833-2844. https://doi.org/10.1109/tmtt.2020.2975637

[12] Kelly, N. and Zhu, A. (2018) Direct Error-Searching Spsa-Based Model Extraction for Digital Predistortion of RF Power Amplifiers. *IEEE Transactions on Microwave Theory and Techniques*, **66**, 1512-1523. https://doi.org/10.1109/tmtt.2017.2748128

[13] Li, Y., Wang, X. and Zhu, A. (2020) Sampling Rate Reduction for Digital Predistortion of Broadband RF Power Amplifiers. *IEEE Transactions on Microwave Theory and Techniques*, **68**, 1054-1064. https://doi.org/10.1109/tmtt.2019.2944813

[14] Wang, S., Roger, M., Sarrazin, J. and Lelandais-Perrault, C. (2020) Augmented Iterative Learning Control for Neural-Network-Based Joint Crest Factor Reduction and Digital Predistortion of Power Amplifiers. *IEEE Transactions on Microwave Theory and Techniques*, **68**, 4835-4845. https://doi.org/10.1109/tmtt.2020.3011152

[15] Jaraut, P., Abdelhafiz, A., Chenini, H., Hu, X., Helaoui, M., Rawat, M., *et al.* (2021) Augmented Convolutional Neural Network for Behavioral Modeling and Digital Predistortion of Concurrent Multiband Power Amplifiers. *IEEE Transactions on Microwave Theory and Techniques*, **69**, 4142-4156. https://doi.org/10.1109/tmtt.2021.3075689

[16] Lu, Q., Meng, F., Yang, N. and Yu, C. (2018) A Uniform Digital Predistorter for Concurrent Multiband Envelope Tracking RF Power Amplifiers with Different Envelopes. *IEEE Transactions on Microwave Theory and Techniques*, **66**, 3947-3957. https://doi.org/10.1109/tmtt.2018.2857828

[17] Zhai, J., Zhang, Q., Niu, J., Zhang, L., Yu, Z., Zhou, J., *et al.* (2020) A 2-D Simplified Memory Polynomial Model for Concurrent Dual-Band Power Amplifiers. *IEEE Microwave and Wireless Components Letters*, **30**, 761-763. https://doi.org/10.1109/lmwc.2020.3003002

[18] Cao, W., Wang, S., Landin, P.N. and Eriksson, T. (2022) Low-Complexity Digital Predistortion of Concurrent Multiband RF Power Amplifiers. *IEEE Transactions on Microwave Theory and Techniques*, **70**, 4308-4317. https://doi.org/10.1109/tmtt.2022.3193907

[19] Liu, Z., Hu, X., Xu, L., Wang, W. and Ghannouchi, F.M. (2022) Low Computational Complexity Digital Predistortion Based on Convolutional Neural Network for Wideband Power Amplifiers. *IEEE Transactions on Circuits and Systems II: Express Briefs*, **69**, 1702-1706. https://doi.org/10.1109/tcsii.2021.3109973

[20] Li, Y., Wang, X. and Zhu, A. (2021) Complexity-Reduced Model Adaptation for Digital Predistortion of RF Power Amplifiers with Pretraining-Based Feature Extraction. *IEEE Transactions on Microwave Theory and Techniques*, **69**, 1780-1790. https://doi.org/10.1109/tmtt.2020.3039788

[21] Noweir, M., Zhou, Q., Kwan, A., Valivarthi, R., Helaoui, M., Tittel, W., *et al.* (2018) Digitally Linearized Radio-Over Fiber Transmitter Architecture for Cloud Radio Access Network's Downlink. *IEEE Transactions on Microwave Theory and Techniques*, **66**, 3564-3574. https://doi.org/10.1109/tmtt.2018.2819665

[22] Noweir, M., Helaoui, M., Oblak, D., Chen, W. and Ghannouchi, F.M. (2021) Linearization of Radio-over-Fiber Cloud-Ran Transmitters Using Pre- and Post-Distortion Techniques. *IEEE Photonics Technology Letters*, **33**, 339-342. https://doi.org/10.1109/lpt.2021.3062761

[23] Pereira, L.A.M., Mendes, L.L., Bastos-Filho, C.J.A. and Arismar Cerqueira, S. (2022) Linearization Schemes for Radio over Fiber Systems Based on Machine Learning Algorithms. *IEEE Photonics Technology Letters*, **34**, 279-282. https://doi.org/10.1109/lpt.2022.3151616

[24] Xie, X., Hui, M., Liu, T. and Zhang, X. (2018) Hybrid Linearization of Broadband Radio-over-Fiber Transmission. *IEEE Photonics Technology Letters*, **30**, 692-695. https://doi.org/10.1109/lpt.2018.2812745

[25] Li, P., Pan, W., Huang, L., Zou, X., Pan, Y., Zhou, Q., *et al.* (2019) Multi-If-over-Fiber Based Mobile Fronthaul with Blind Linearization and Flexible Dispersion Induced Bandwidth Penalty Mitigation. *Journal of Lightwave Technology*, **37**, 1424-1433. https://doi.org/10.1109/jlt.2019.2894686

[26] Noweir, M., Helaoui, M., Oblak, D. and Ghannouchi, F.M. (2021) Linearized Full Duplex Radio-over-Fiber-over-Space Mixerless Transceiver Architecture. *IEEE Photonics Technology Letters*, **33**, 113-116. https://doi.org/10.1109/lpt.2020.3047001

[27] Hadi, M.U., Traverso, P.A., Tartarini, G., Venard, O., Baudoin, G. and Polleux, J. (2019) Digital Predistortion for Linearity Improvement of VCSEL-SSMF-Based Radio-over-Fiber Links. *IEEE Microwave and Wireless Components Letters*, **29**, 155-157. https://doi.org/10.1109/lmwc.2018.2889004

[28] Pereira, L.A.M., Mendes, L.L., Bastos-Filho, C.J.A. and Jr, A.C.S. (2022) Machine Learning-Based Linearization Schemes for Radio over Fiber Systems. *IEEE Photonics Journal*, **14**, 1-10. https://doi.org/10.1109/jphot.2022.3210454

[29] Zheng, R., Chan, E.H.W., Wang, X., Feng, X. and Guan, B. (2019) Linearized Single Sideband Modulation Link with High SFDR Performance. *IEEE Photonics Technology Letters*, **31**, 299-302. https://doi.org/10.1109/lpt.2019.2892653

[30] Tang, W., Hui, M., Liu, T., Shen, D. and Zhang, X. (2018) A Simple Envelope-Assisted RF/IF Digital Predistortion Model for Broadband ROF Fronthaul Transmission. *Journal of Lightwave Technology*, **36**, 4305-4311. https://doi.org/10.1109/jlt.2018.2846883

[31] Li, P., Pan, W., Zou, X., Bai, W., Pan, Y., Han, X., *et al.* (2021) Fast Self-Adaptive Generic Digital Linearization for Analog Microwave Photonic Systems. *Journal of Lightwave Technology*, **39**, 7894-7907. https://doi.org/10.1109/jlt.2021.3076821

[32] Chen, Y. and Chen, Y. (2022) Linearization for Microwave Photonic OFDM Transmission Systems Using an Iterative Algorithm Based on FEC Mechanism. *Journal of Lightwave Technology*, **40**, 5013-5020. https://doi.org/10.1109/jlt.2022.3173339

[33] Wang, Y., Zhang, H., Wang, D., Zhou, T., Yang, F., Yang, D., *et al.* (2019) Microwave Photonic Link with Flexible Even-Order and Third-Order Distortion Suppression. *IEEE Journal of Quantum Electronics*, **55**, Article ID: 8000209.

https://doi.org/10.1109/jqe.2019.2903490

[34] Wang, F., Shi, S. and Prather, D.W. (2019) LTE Signal Transmission over a Linearized Analog Photonic Link with High Fidelity. *IEEE Photonics Journal*, **11**, Article ID: 7204909. https://doi.org/10.1109/jphot.2019.2905100

[35] Zhong, L., Zou, Y., Zhang, S., Dai, X., Zhang, J., Cheng, M., *et al.* (2022) An Snr-Improved Transmitter of Delta-Sigma Modulation Supported Ultra-High-Order QAM Signal for Fronthaul/Wifi Applications. *Journal of Lightwave Technology*, **40**, 2780-2790. https://doi.org/10.1109/jlt.2022.3147059

[36] Shen, C., He, S., Zhu, X., Peng, J. and Cao, T. (2020) A 3.3-4.3-Ghz High-Efficiency Broadband Doherty Power Amplifier. *IEEE Microwave and Wireless Components Letters*, **30**, 1081-1084. https://doi.org/10.1109/lmwc.2020.3022356

[37] Gan, D., Shi, W., He, S., Gao, Y. and Naah, G. (2020) Broadband Doherty Power Amplifier with Transferable Continuous Mode. *IEEE Access*, **8**, 99485-99494. https://doi.org/10.1109/access.2020.2997826

[38] Liu, X., Chen, W. and Feng, Z. (2021) Broadband Digital Predistortion Utilizing Parallel Quasi-Wiener-Hammerstein Model with Extended Dynamic Range. 2021 *IEEE MTT-S International Wireless Symposium* (*IWS*), Nanjing, 23-26 May 2021, 1-3. https://doi.org/10.1109/iws52775.2021.9499484

[39] Chen, W., Liu, X., Chu, J., Wu, H., Feng, Z. and Ghannouchi, F.M. (2022) A Low Complexity Moving Average Nested GMP Model for Digital Predistortion of Broadband Power Amplifiers. *IEEE Transactions on Circuits and Systems I: Regular Papers*, **69**, 2070-2083. https://doi.org/10.1109/tcsi.2022.3150408

[40] Li, Y. and Zhu, A. (2020) On-Demand Real-Time Optimizable Dynamic Model Sizing for Digital Predistortion of Broadband RF Power Amplifiers. *IEEE Transactions on Microwave Theory and Techniques*, **68**, 2891-2901. https://doi.org/10.1109/tmtt.2020.2982165

[41] Yu, C., Hou, D., Sun, H., Meng, F., Zhu, X., Zhai, J., *et al.* (2017) A Reconfigurable In-Band Digital Predistortion Technique for mmWave Power Amplifiers Excited by a Signal with 640 MHz Modulation Bandwidth. 2017 47*th European Microwave Conference* (*EuMC*), Nuremberg, 10-12 October 2017, 1046-1049. https://doi.org/10.23919/eumc.2017.8231025

[42] Abe, T. and Yamao, Y. (2018) Band-Split Parallel Signal Processing DPD for Nonlinear Compensation of Broadband RF Signal. 2018 15*th International Symposium on Wireless Communication Systems* (*ISWCS*), Lisbon, 28-31 August 2018, 1-5. https://doi.org/10.1109/iswcs.2018.8491244

[43] Kwan, A.K., Younes, M., Ghannouchi, F.M., Zhang, S., Chen, W., Darraji, R., *et al.* (2014) Concurrent Multi-Band Envelope Modulated Power Amplifier Linearized Using Extended Phase-Aligned DPD. *IEEE Transactions on Microwave Theory and Techniques*, **62**, 3298-3308. https://doi.org/10.1109/tmtt.2014.2365816

[44] Tang, W. (2017) Envelope-Assisted RF Digital Predistortion for Broadband Radio-over-Fiber Systems with RF Power Amplifiers. Master's Thesis, Concordia University. https://spectrum.library.concordia.ca/view/creators/Tang=3AWeijie=3A=3A.html